genesis 31:43–53 (2001)

ARTICLE

The *eyeless* Mouse Mutation *(ey1)* Removes an Alternative Start Codon from the *Rx/rax* Homeobox Gene

Priscilla Tucker,[1] Lois Laemle,[2] Amanda Munson,[3] Shami Kanekar,[4] Edward R. Oliver,[3] Nadean Brown,[5] Hans Schlecht,[2] Monica Vetter,[4] and Tom Glaser[3]*

[1]Museum of Zoology and Department of Ecology and Evolutionary Biology, University of Michigan, Ann Arbor, Michigan
[2]Departments of Anatomy, Cell Biology and Molecular Medicine and Ophthalmology, University of Medicine and Dentistry of New Jersey, Newark, New Jersey
[3]Departments of Internal Medicine and Human Genetics, University of Michigan, Ann Arbor, Michigan
[4]Department of Neurobiology and Anatomy, University of Utah, Salt Lake City, Utah
[5]Children's Memorial Institute for Education and Research, Department of Pediatrics, Northwestern University, Chicago, Illinois

Received 1 August 2001; Accepted 2 August 2001

Summary: The eyeless inbred mouse strain ZRDCT has long served as a spontaneous model for human anophthalmia and the evolutionary reduction of eyes that has occurred in some naturally blind mammals. ZRDCT mice have orbits but lack eyes and optic tracts and have hypothalamic abnormalities. Segregation data suggest that a small number of interacting genes are responsible, including at least one major recessive locus, *ey1*. Although predicted since the 1940s, these loci were never identified. We mapped *ey1* to chromosome 18 using an F2 genome scan and there found a Met10→Leu mutation in *Rx/rax*, a homeobox gene that is expressed in the anterior headfold, developing retina, pineal, and hypothalamus and is translated via a leaky scanning mechanism. The mutation affects a conserved AUG codon that functions as an alternative translation initiation site and consequently reduces the abundance of Rx protein. In contrast to a targeted *Rx* null allele, which causes anophthalmia, central nervous system defects, and neonatal death, the hypomorphic M10L allele is fully viable. genesis 31:43–53, 2001. © 2001 Wiley-Liss, Inc.

Key words: *Rx; rax;* homeobox; eye development; start codon; mouse; mutation; protein translation; leaky scanning

INTRODUCTION

The phenotype of ZRDCT mice (Fig. 1a) is similar to human clinical anophthalmia (Duke-Elder, 1964; Kohn *et al.,* 1988) and the rudimentary development of eyes in some fossorial (subterranean) mammals (Cooper *et al.,* 1993). More than 90% of mice in this inbred strain have no eyes or optic tracts, although the eyelids, bony orbits, palpebral conjunctivae, Harderian glands, and periocular soft tissues are intact (Chase and Chase, 1941; Silver and Hughes, 1974). Higher visual centers in the brain, including the lateral geniculate nuclei and visual cortex, form normal projections and exhibit normal topographic connectivity but are attenuated (Chase, 1945; Godement *et al.,* 1979; Katz *et al.,* 1981; Olavarria and van Sluyters, 1984; Rhoades *et al.,* 1985). The hypothalamus has variably distorted anatomy (Laemle and Rusa, 1992; Silver, 1977) and there are intrinsic circadian rhythm disturbances (Faradji-Prevautel *et al.,* 1990; Laemle and Ottenweller, 1998). The remaining 10% of ZRDCT mice have one or two small eyes with colobomatous defects and no optic nerve (Silver *et al.,* 1984). The phenotype is first apparent during lens induction at day E10. The optic vesicles emerge normally from the anterior neural tube but are reduced in size and contact poorly with the surface ectoderm (Chase and Chase, 1941; Harch *et al.,* 1978; Silver and Hughes, 1974; Webster *et al.,* 1984). In some embryos, there is a small displaced lens placode and limited crystallin synthesis (Konyukhov *et al.,* 1978; Zwaan and Silver, 1983). The eyeless trait is one of the first developmental defects and first examples of multifactorial inheritance described in laboratory mice.

In crosses between ZRDCT and most other laboratory strains, the eyeless phenotype behaves as a polygenic trait. F1 mice are normal, but 10–13% of F2 intercross and 20–25% of N2 backcross progeny are affected (Beck, 1963; Chase, 1942). On the basis of these experiments, Chase (1944) postulated a major recessive eyeless determinant *(ey1)* and a modifier *(ey2)* with partial dominance. In this study, we test this model, identify the *ey1* mutation, and characterize its molecular properties in detail.

* Correspondence to: Tom Glaser, 4510 MSRB I, Box 0650, 1150 West Medical Center Drive, Ann Arbor, MI 48109-0650.
E-mail: tglaser@umich.edu

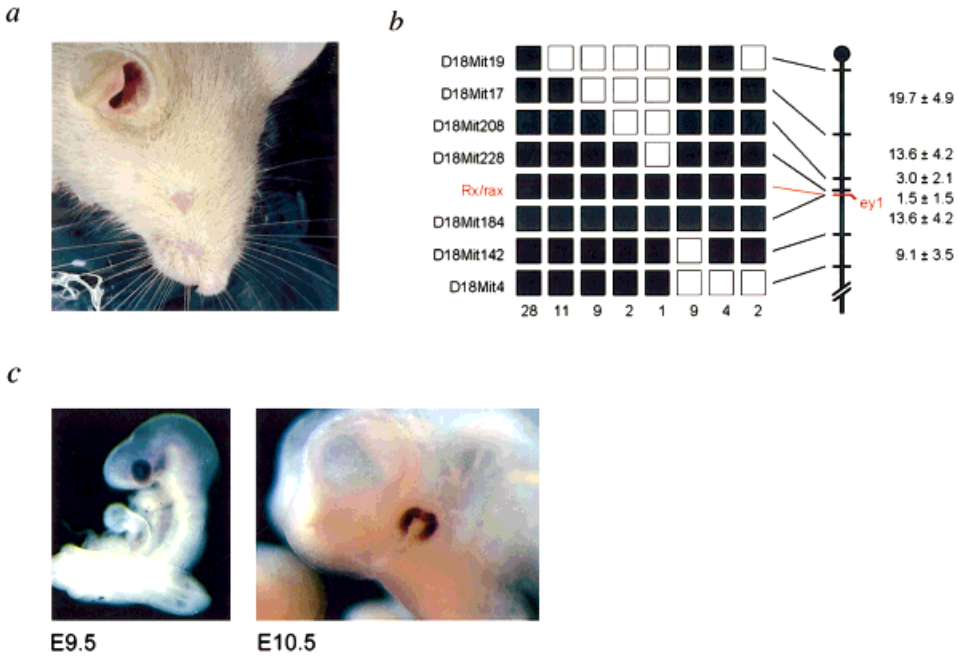

FIG. 1. Mapping *ey1* in relation to *Rx/rax*. **(a)** Phenotype of the ZRDCT mice. **(b)** Segregation data from 33 eyeless (ZRDCT × CAST/Ei) F2 progeny localize *ey1* on chromosome 18 near *Rx/rax*. Recombinant and nonrecombinant chromosomes are represented vertically, along with the total number observed in each class. A genetic map of MMU18 derived from these data is shown on the right. Distances (cM ± SE) are similar to those reported previously (Dietrich *et al.,* 1994). An additional 21 eyeless F2 mice were typed at *Rx/rax* and *D18Mit184*. No recombination was observed between these two markers and *ey1*. ■, ZRDCT; □, CAST/Ei genotypes. **(c)** Whole-mount in situ hybridization showing *Rx/rax* mRNA in the optic vesicle of E9.5 and optic cup of E10.5 embryos. Expression in the optic cup is confined to the presumptive neural retina and does not extend into the choroid fissure.

RESULTS

To map *ey1*, we performed a pooled genome scan (Taylor *et al.,* 1994) using F2 progeny derived from ZRDCT and CAST/Ei, an inbred strain of the relatively divergent subspecies *Mus musculus castaneus.* Among 2,316 F2 offspring, we observed 2,109 normal (91.1%), 153 intermediate (6.6%), and 54 bilaterally eyeless (2.3%) mice. The proportion of affected F2 progeny is thus between 1/8 and 1/16. These ratios are similar to segregation data reported for crosses between ZRDCT and conventional laboratory mice (Beck, 1963; Chase, 1942; Chase, 1944). By screening two pools of bilaterally anophthalmic F2 mice with multiple SSLP (simple sequence length polymorphism) markers, we detected linkage between *ey1* and chromosome 18. We then singly tested all 54 eyeless F2 mice using additional markers and a fragment length polymorphism in the second intron of *Rx/rax*, a retinal homeobox gene previously mapped to this region (Furukawa *et al.,* 1997) (Fig. 1b). No recombination was observed between *Rx* and *ey1*, suggesting that they are located within 2.8 cM (95% CI for $n = 108$ meioses, with a LOD score in favor of linkage >30).

The *Rx* gene is an attractive candidate for *ey1* for several reasons. First, it encodes a 342 amino acid transcription factor with four evolutionarily conserved motifs: a paired-class homeodomain, a C-terminal OAR (paired tail) domain (Furukawa *et al.,* 1997; Mathers *et al.,* 1997), an octapeptide motif near the N-terminus, and a segment of high sequence conservation just beyond the homeobox termed the Rx domain (Fig. 2a). Multiple *Rx* homologues are known in the zebrafish, medaka, chicken, and frog, and these can be divided into two paralogous groups (Casarosa *et al.,* 1997; Chuang *et al.,* 1999; Deschet *et al.,* 1999; Ohuchi *et al.,* 1999). Homeodomain genes of this type are well known to regulate morphogenesis. Second, *Rx* is one of the earliest retinal patterning genes to be expressed, preceding *Pax6* and *Chx10*. It first appears at day E7.5 in regions of the anterior neural plate and headfold that are fated to become retina and is expressed most intensely in the optic vesicle and cup between days E9 and E11 (Fig. 1c). *Rx* is relatively specific to the developing eye but also appears in the ventral forebrain, presumptive hypothalamus, and posterior pituitary (Furukawa *et al.,* 1997; Mathers *et al.,* 1997). This expression pattern has been generally well conserved during vertebrate evolution. A *Drosophila* homologue is expressed in the developing brain and clypeolabrum but does not have a major role in eye morphogenesis (Eggert *et al.,* 1998). Third, *Rx* is required for optic vesicle formation. Mice homozygous for an *Rx* null allele are anophthalmic but also die at birth with major central nervous system and craniofacial defects (Mathers *et al.,* 1997).

To evaluate *Rx* as a candidate for *ey1*, we determined its genomic structure and DNA sequence in ZRDCT, CAST/Ei, and two conventional laboratory strains (Fig. 2b). The mouse *Rx* gene spans 5.6 kb and is divided into three exons. We discovered a single nucleotide change in the coding region that is unique to ZRDCT mice. The change (ATG→TTG) causes an M10L amino acid substitution and destroys an *Nco*I restriction site (Fig. 2b, c). To confirm the relationship between *Rx*(M10L) and *ey1*, we surveyed a variety of laboratory strains, wild-caught mice, and other *Mus* species by PCR and *Nco*I digestion (Fig. 2d). The M10L mutation was found in ZRDCT mice from different sources but was absent from all other mice tested, including C57BL strains which have a 4-10%

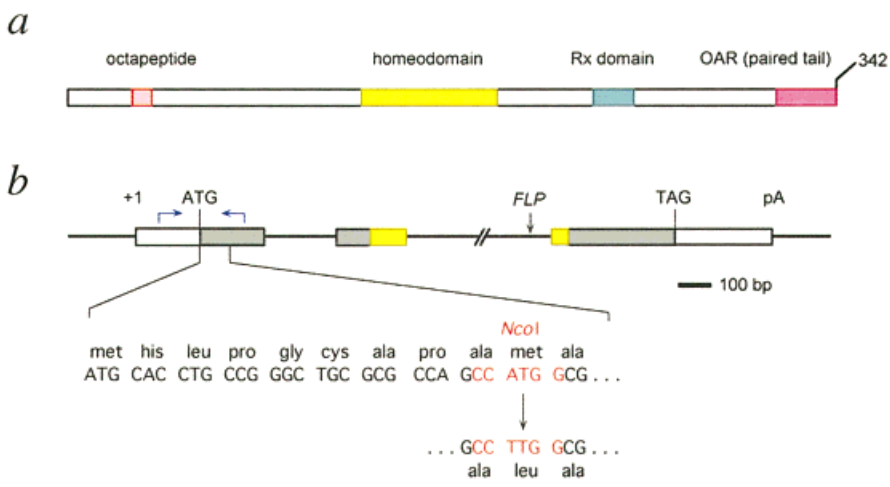

FIG. 2. The *Rx*(M10L) mutation. **(a)** Structure of the mouse Rx protein showing four conserved motifs. **(b)** Genomic map of *Rx* showing three exons, the 3-bp fragment length polymorphism (FLP) used for linkage mapping, the PCR primers used for mutation screening (blue arrows), and the M10L mutation. Homeobox segments (yellow) are indicated within the coding region (gray). The relevant ZRDCT nucleotide sequence is shown below the wild type, along with the *Nco*I site (red text). Complete genomic sequence data are available from Genbank. **(c)** Southern analysis of *Rx* confirming the loss of an *Nco*I restriction site in ZRDCT mice. C, C3H/HeJ; B, C57BL/6J; Z, ZRDCT. **(d)** Survey of selected mouse strains for the *Rx*(M10L) mutation. PCR products from exon1 were digested with *Nco*I and electrophoresed through a 3% agarose gel. Similar results were obtained with DNA samples from other strains and wild-caught mice (see Methods).

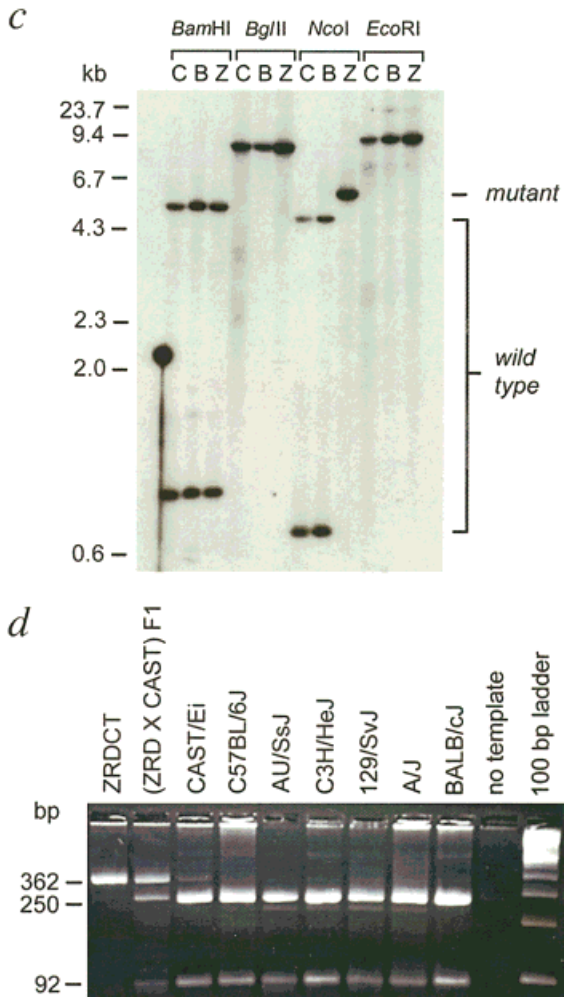

background frequency of anophthalmia (Chase, 1942; Pierro and Spiggle, 1967; Robinson *et al.,* 1993; Smith *et al.,* 1994) and may share a common ancestry (Beck *et al.,* 2000; Chase, 1944) with the extinct B strain that is the progenitor of ZRDCT. Moreover, a methionine codon is present at position 10 in *Rx* genes of all other mammals examined, including humans, rats, and six additional phylogenetically diverse rodent species, and at the equivalent position in *Rx* genes of fish, amphibians, and birds (Fig. 3a, left, and data not shown). This methionine codon thus exhibits a level of evolutionary sequence conservation exceeding that found among vertebrate *Rx* homeodomains, which are ≥96% identical. It is thus improbable that the L10 allele is segregating within mouse populations as a neutral polymorphism. We conclude that *Rx*(M10L) is most likely the *ey1* determinant.

In principle, the M10L mutation could affect intrinsic properties of the Rx protein or the efficiency of translation initiation. Although this methionine codon appears to have been selectively retained among vertebrates for at least 400 million years, the mutation itself is a conservative amino acid substitution (an exchange between hydrophobic residues) and does not occur within a previously defined functional domain. The identity of the *Rx* start codon is also unclear, since the sequence surrounding the first in-frame methionine codon (M1) conforms poorly to the consensus for translation initiation compared with M10. In particular, the M1 site lacks a G at position +4 and a purine at position −3, which are considered critical for ribosome recognition via a cap-dependent scanning mechanism (Kozak, 1996). These three sequence characteristics are common to all vertebrate *Rx* genes (Fig. 3a, right). The choice of initiation site can also be significantly influenced by mRNA secondary structure (Kozak, 1990). To determine the true initiation site and the effect of the M10L mutation in vivo, we compared the size of Rx-myc fusion proteins

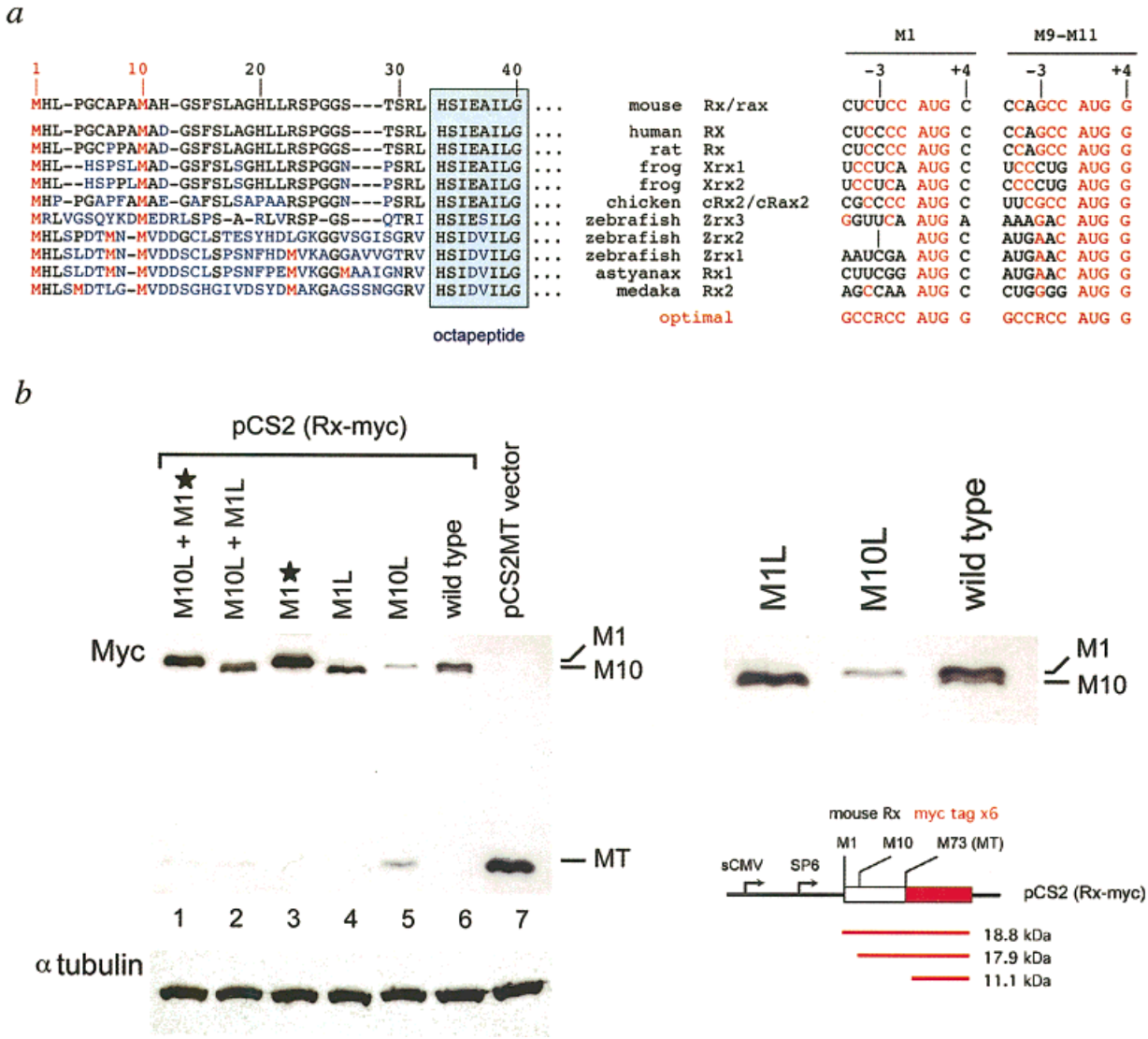

FIG. 3. The *Rx*(M10L) mutation affects translation initiation. **(a)** Left: N-terminal alignment of vertebrate Rx proteins. Sequences were obtained from GenBank and are numbered in relation to mouse Rx/rax. Methionines (red) and residues that differ from mouse Rx/rax (blue) are indicated. The methionine at position 9, 10, or 11 has been conserved during evolution. Right: Comparison of M1 and M9–11 translational start sites in vertebrate *Rx* mRNAs. The optimal sequence for translation initiation (Kozak, 1996) is shown below each alignment, and the nucleotide matches are indicated in red text. In each case, the downstream site is a significantly more favorable context than M1. **(b)** Western analysis of Rx-myc fusion polypeptides translated in vivo (transfected 293T cells). Left: Western blot showing Myc-tagged proteins initiating at M1, M10, or M73 (within the pCS2MT vector). Lanes 1 and 2 contain mixtures of cell extracts from lanes 3+5 and lanes 4+5, respectively. The α-tubulin blot below is a loading control. Right: Magnified view of Myc Western blot (lanes 4–6). The diagram below shows the framework pCS2MT expression construct and predicted protein products. Wild-type *Rx* mRNA starts translation at both M1 and M10 codons. The M1★ mRNA starts translation exclusively at M1, whereas the M1L mRNA starts translation exclusively at M10. The M10L mutation eliminates the shorter product and decreases overall translation efficiency. MT, myc tag; ★, optimal start site.

translated in cells transfected with mutant or wild-type plasmid constructs (Fig. 3b). The fusion mRNAs contain 5′ UTR sequences and the first 66 potential codons of the mouse *Rx* gene. Proteins initiating at codons 1 or 10 are predicted to be 18.8 or 17.9 kDa, respectively. We also tested control constructs containing an M1L substitution or an optimal initiation sequence at M1. When the wild-type fusion construct was tested, both methionine codons were utilized as translation start sites (lane 6), consistent with a leaky scanning model (Kozak, 1995). The relative abundance of these two proteins presumably reflects the balance between competing factors that favor initiation at M1 (proximity to the 5′ m7G cap) versus M10 (context superiority for engaging the 40S ribosomal subunit). The M10L mutation prevented initiation at codon 10 and significantly lowered the efficiency of *Rx* translation overall (compare lanes 5 and 6). The decrease in translation efficiency was demonstrated

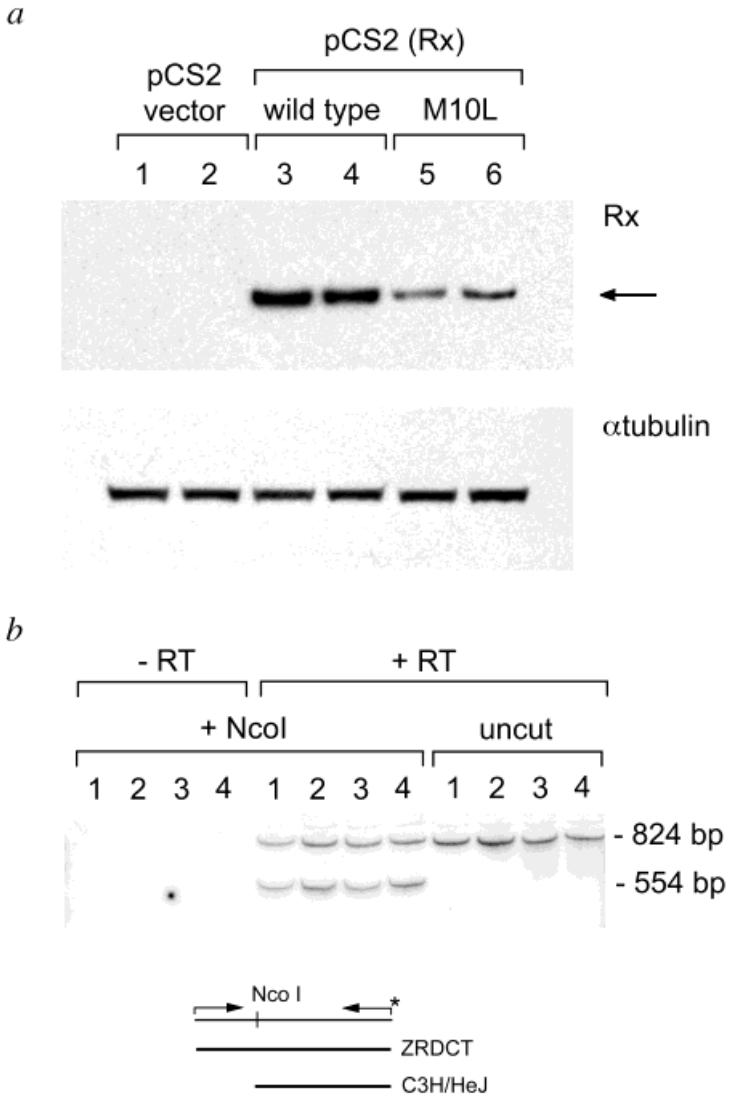

FIG. 4. The M10L mutation reduces the abundance of Rx protein, but not *Rx* mRNA. **(a)** Western analysis of HER10 retinal cells expressing full-length wild-type or M10L mutant *Rx* mRNAs. Top: The level of Rx polypeptide (36 kDa, arrow) is decreased approximately four-fold in duplicate cultures transfected with pCS2(*Rx*M10L) compared with wild-type pCS2(*Rx*) plasmid. The M1- and M10-initiated Rx isoforms are not resolved in this gel. Bottom: Endogenous α-tubulin (57 kDa) shows equivalent protein loading. **(b)** M10L and wild-type *Rx* transcripts are amplified equally from E14.5 (C3H/HeJ × ZRDCT) F1 embryos. An RT-PCR spanning exons 1–3 was performed on total head RNA from four littermates (lanes 1–4). The wild-type product is cleaved by *Nco*I (554 bp) but the mutant product is resistant (824 bp). These alleles are equally represented in the heterozygotes, suggesting that the mRNAs are similarly expressed and stable. No product was amplified in the absence of reverse transcriptase.

most clearly by the appearance of an 11.1 kDa immunoreactive protein; this reflects ribosome scanning past both codons 1 and 10 and initiation at the first in-frame AUG codon of the pCS2MT vector (compare lanes 5 and 7). In contrast, the reciprocal M1L mutation prevented initiation at codon 1 in vivo but did not significantly lower overall translation (lane 4).

To assess the effect of the M10L mutation quantitatively in the context of the full-length *Rx* transcript, we compared Rx protein levels in fetal retinal cells that were transfected with either a mutant or wild-type expression plasmid (Fig. 4a). These plasmids express the entire *Rx* mRNA, including the open reading frame and UTRs, but differ by a single nucleotide. We observed a significant reduction in the abundance of Rx protein (compare lanes 3–6), which can best be explained by a decrease in translation efficiency. The mutation does not destabilize *Rx* mRNA, since wild-type and M10L transcripts were equally abundant in this experiment (data not shown) and in heterozygous (C3H/HeJ × ZRDCT) F1 embryos (Fig. 4b).

Finally, as a further functional test, we compared the activity of Rx isoforms in a *Xenopus* RNA microinjection assay (Andreazzoli *et al.,* 1999; Mathers *et al.,* 1997). We first tested an M9L substitution in frog *Xrx1* cDNA that is equivalent to the ZRDCT mouse *Rx* mutation. When injected into a D.1 blastomere of an 8-cell frog embryo, M9L and wild-type *Xrx1* RNAs were both capable of inducing ectopic pigmented epithelium, although neither caused significant expansion of neural retina (data not shown). We then compared the activity of mouse Rx proteins initiating at M1 or M10 and M1-initiated proteins with methionine or leucine at codon 10. We observed a wide range of abnormal phenotypes on the injected sides, including small or absent eyes, cyclopia, retinal disruption, and ectopic pigmented epithelium along the optic stalk (data not shown). These results confirm that eye morphogenesis is sensitive to Rx dos-

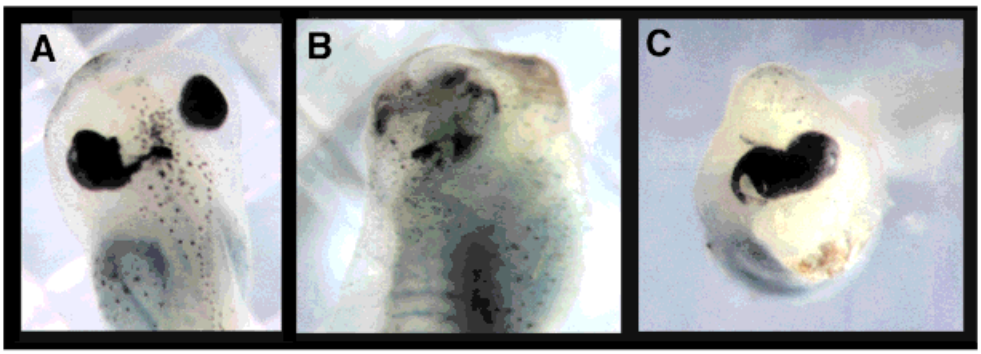

FIG. 5. Phenotypes resulting from overexpression of mouse *Rx* in *Xenopus* (shown at stages 39–41). RNA was injected into one dorsal blastomere of each 8-cell embryo. (**A**) Abnormal pigmentation; (**B**) missing eye; (**C**) eyes joined at midline

age. (Fig. 5) (Table 1). However, there was no significant qualitative difference between the mutant and wild-type isoforms or between proteins initiating at M1 or M10 in their effect on frog eye development. The *ey1* mutation thus does not grossly alter the intrinsic biological properties of Rx proteins.

DISCUSSION

Taken together, our findings show that ribosomes frequently bypass the suboptimal M1 site and initiate at the downstream M10 codon, producing two Rx proteins that differ by nine amino acids from one mRNA. Although rare, translational control by alternative start codon usage from a single transcript can provide a further opportunity to regulate protein function (Cornelis *et al.,* 2000; Hann *et al.,* 1988; Liu *et al.,* 1997; Markussen *et al.,* 1995; Sedman and Mertz, 1988). While this remains a possibility for *Rx*, and the M10L mutation does delete the shorter isoform, we believe the primary effect of *ey1* is a quantitative reduction in the synthesis of Rx polypeptide. This effect was likely to be significantly greater than two-fold a priori, since mice heterozygous for a targeted *Rx* null allele are phenotypically normal (Mathers *et al.,* 1997). Indeed, our data suggest that the M10L mutation decreases *Rx* translation by at least four-fold (Figs. 3b, 4a). This result, together with (1) the meiotic linkage between *Rx* and *ey1*; (2) the unique M10L sequence alteration in the ZRDCT strain; (3) the deep evolutionary conservation of M10; (4) the established role of Rx and homeodomain proteins generally in eye development; and (5) the specific effect of M10L on alternative initiation, strongly suggests that *Rx*(M10L) can be equated with *ey1*. A potentially similar but less profound reduction in the efficiency of translation initiation was reported for a mutation in codon 2 of the human androgen receptor gene that causes a hypomorphic phenotype (Choong *et al.,* 1996). In contrast, missense mutations affecting solitary start codons generally cause a complete loss of function (Cheadle *et al.,* 1994; Tsujino *et al.,* 1994; Waye *et al.,* 1997). To our knowledge, *Rx*(M10L) is the first example of a constitutional mutation affecting an alternative start codon.

Our findings explain a number of previous observations regarding *Rx* and this strain. First, the eye and hypothalamic phenotypes of ZRDCT mice closely match the *Rx* expression pattern. Second, the M10L substitution is compatible with the behavior of *ey1* as a hypomorphic allele. This is manifest during embryogenesis by a graded reduction in the size of the optic vesicle and in the adult phenotype. Third, explant data show an intrinsic growth defect in the neural retina of ZRDCT embryos but not in lens primordia (Koniukhov and Iakovlev, 1986). Within the mouse eye, *Rx* expression is limited to the optic cup and neural retina and is relatively independent of *Pax6* (Bernier *et al.,* 2000; Zhang *et al.,* 2000; NB and TG, unpublished observations). Accordingly, microphthalmia or anophthalmia can result from mutations in patterning genes that are expressed in the optic cup, lens, or both (Breitman *et al.,* 1987; Burmeister *et al.,* 1996; Ferda Percin *et al.,* 2000; Hill *et al.,* 1991; Hodgkinson *et al.,* 1993).

Approximately one-half to two-thirds of the F2 mice homozygous for the *Rx*(M10L) mutation have normally sized eyes. This conclusion follows from the phenotypic segregation data, which show fewer affected mice than the 25% expected for a single recessive mendelian factor; the absence of excess perinatal lethality among the F2 progeny and parental ZRDCT mice; and the finding of M10L homozygotes in the normal F2 progeny class (data not shown). The *Rx*(M10L) mutation is thus necessary but not sufficient to produce anophthalmia in the ZRDCT strain. This decreased penetrance and the phenotypic variability among affected F2 mice are reminiscent of anophthalmia and microphthalmia in some human pedigrees (Bateman, 1984). Our results suggest that *RX* mutations may underlie some of these human disorders (Voronina and Mathers, 2000). The inheritance pattern also suggests that unlinked modifier gene(s), are likely to interact with *Rx* in a developmental pathway for the eye or otherwise control the threshold for phenotypic expression of *ey1*. Although a single modifier (*ey2*)

Table 1
Phenotypes Observed Following Overexpression of Mouse Rx *in* Xenopus *Embryos**

	Rx (wild type)		Rx (M10L)	
Phenotype	No.	%	No.	%
Pigmentation abnormalities	114	62	87	39
Small or missing eyes	30	16	36	16
Eyes joined along midline	6	3	9	4
Other abnormal phenotypes[a]	3	2	11	5
Normal	32	17	81	36
Total	185		224	

*RNA (10 pg) was transcribed in vitro from wild-type or M10L pCS2(*Rx*) plasmids, injected into one dorsal blastomere of an 8-cell embryo, and evaluated at stage 39–41. Although there was no qualitative difference between mutant and wild type, the M10L RNA was generally less potent, consistent with decreased translation efficiency. Similar results were observed with wild-type and M9L *Xrx1* RNAs.

[a]Other phenotypes we observed include: no eyes, with random pigmentation along the midline of the anterior head (most common); one eye displaced anteriorly at midline; and no eyes, with no pigmentation.

was originally proposed by Chase (1944), the actual number of modifiers cannot be determined from segregation data alone (Beck, 1963; Wright, 1968), since their individual dominance characteristics and potential epistatic relationships are unknown. This number, however, is likely to be small. The discovery of *ey1* provides a basis to identify these genes. Comparable modifier loci have been defined for mutations affecting limb morphogenesis (Johnson *et al.,* 1995; Sidow *et al.,* 1997) and other eye diseases (Bone-Larson *et al.,* 2000; Chang *et al.,* 1999; Kajiwara *et al.,* 1994).

Finally, as a synthetic trait involving a partial loss-of-function mutation, the ZRDCT phenotype is suggestive of the quantitative, polygenic interactions that underlie the appearance and loss of morphological characteristics during evolution (Grenier and Carroll, 2000; Wright, 1968). Extreme eye reduction is typical of troglobitic (cave-dwelling) and fossorial species, which are found within every class of vertebrates except birds. Adaptive loss of function (Olson, 1999) involving quantitative changes in the activity of genes such as *Rx* may thus contribute to ocular regression in naturally blind species (Cooper *et al.,* 1993; Wilkens, 1971; Yamamoto and Jeffery, 2000).

METHODS

Mice

The inbred ZRDCT strain *(aa bb dd pp)* was derived (Beck, 1963) from the original B strain *(bb dd)* of Herman Chase, who received founders directly from C.C. Little in 1938 (Chase, 1942). The eyeless phenotype was first noted at the Jackson Laboratory within a colony of strain R mice, among progeny of a wide cross, and was positively selected by Little during the initial breeding (Chase, 1949; Snell, 1941). To generate intersubspecific F2 mice, we crossed eyeless ZRDCT males and females to inbred *Mus musculus castaneus* mice (CAST/Ei, obtained from the Jackson Laboratory) and intercrossed the resulting F1 progeny. Phenotypes were scored two weeks after birth when the eyelids had opened. Eyes were classified according to Chase (1942) as normal, small, or absent, and individual F2 pups as normal, eyeless (bilateral anophthalmia), or intermediate (microphthalmia or unilateral anophthalmia). In cases where the lids remained closed, the conjunctival sacs were explored and generally found to be anophthalmic. For RNA analysis, we crossed ZRDCT males to C3H/HeJ females and recovered F1 embryos on day E14.5 of gestation.

PCR Genotyping

A genome scan was performed using 58 SSLP markers distributed across the autosomes (Dietrich *et al.,* 1994). Genomic DNA from 12 severely affected F2 mice was divided into two equal pools (Taylor *et al.,* 1994). Markers were amplified for 40 cycles using standard PCR conditions and primer pairs (Research Genetics). Short, secondary PCRs (10 cycles) were then performed with one ^{32}P-end-labeled primer and the products separated by electrophoresis through 6% polyacrylamide sequencing gels. F2 pools were compared with ZRDCT, CAST/Ei, and F1 genomic DNA controls. Once linkage was detected, by an enrichment of ZRDCT alleles in the pooled DNA, a larger set of 54 eyeless F2 mice was typed individually using additional markers on chromosome 18.

Rx Gene Analysis

Overlapping segments of mouse *Rx* were amplified from ZRDCT, C3H/HeJ, C57BL/6J, and CAST/Ei genomic DNA by high-fidelity long-range PCR (EXPAND, Roche) using primers designed from the cDNA sequence (Furukawa *et al.,* 1997; Mathers *et al.,* 1997). Betaine (20% v/v MasterAmp, Epicentre) was included in some reactions to improve yield of GC-rich products. Terminal fragments were recovered from *Bam*HI-digested genomic DNA by inverse PCR (Ochman *et al.,* 1990). The amplified products were sequenced directly and used to assemble two *Rx* contigs. These are separated by 2.1 kb and correspond to exons 1–2 and 3 (accession nos. AF319462 and AF319461). To localize *Rx* directly in the F2 cross, we typed a 3-bp insertion in the second intron, using PCR primers 5′-CCTGTGGGTCAGAGAGGATAGCGAC-3′ and 5′-CTGGCGCCTCCACTTAGCCCGTCGG-3′ which span 265 bp. Southern analysis of mouse genomic DNA was performed using a 785-bp 5′ *Rx* cDNA probe (Mathers *et al.,* 1997) and high stringency wash conditions (0.1 × SSC, 65°C). To demonstrate the M10L *Rx* mutation, a 361-bp fragment of exon 1 was amplified using primers 5′-CTAAACTTGCAGCTCCAGCAGCGGG-3′ and 5′-GCCCAGGATGGCTTCGATGCTGTG-3′ and digested with *Nco*I. The wild-type PCR product is cleaved into 269- and 92-bp fragments, but the M10L product is resistant to cleavage. We used this assay to survey normal inbred laboratory mice (A/J, AU/SsJ,

BALB/cJ, CBA/J, C3H/HeJ, C57BL/6J, C57BL/10J, C57BR/cdJ, C57L/J, C58/J, DBA/2J, LT/ChRe, SJL/J, SWR/J, 129/SvJ); *Mus musculus castaneus* (CAST/Ei), *Mus spretus* (SPE/Ei), *Mus musculus molossinus* (MOLF/Ei), and a Peruvian strain (PERA), each obtained as DNA from the Jackson Laboratory; wild-caught *Mus musculus* and *Mus domesticus* from the hybrid zone of Northern Europe (kindly provided by Richard Sage); and eyeless ZRDCT mice from colonies in Rhode Island (Harch *et al.,* 1978) and Moscow (Konyukhov *et al.,* 1978), which have been maintained separately for more than 20 years (kindly provided by Neil Gonsalves and Boris Konyukhov).

RNA Analysis

Whole-mount in situ hybridization was performed on wild-type CD1 mouse embryos as described (Brown *et al.,* 1998) using a 5′ *Rx* cDNA probe (Mathers *et al.,* 1997). To test whether the M10L mutation affects transcript stability, we performed a reverse transcriptase (RT) PCR assay on (C3H/HeJ × ZRDCT) F1 embryos. Total RNA from E14.5 heads was randomly primed and used to amplify 824-bp *Rx* cDNA products spanning exons 1–3 with PCR primers 5′-CTAAACTTGCAGCTCCAGCAGCGGG-3′ and 5′-CTGGCGCCTCCACTTAGCCCGTCGG-3′. The reverse primer was ^{32}P-end-labeled and the PCR was for 30 cycles. Mutant and wild-type transcripts differ by a single nucleotide. Their relative abundance was determined by cleaving the radiolabeled PCR products with *Nco*I and comparing the ratio of 824- and 554-bp allelic fragments after polyacrylamide gel electrophoresis. The two alleles amplified equally in control reactions performed on F1 genomic DNA.

Rx Plasmids

Mouse *Rx* cDNA clones with M10L and M1L mutations (ATG→TTG) or optimal translation initiation sites (Kozak, 1996) M1★ and M10★ (GCCACCATGG) were created by oligonucleotide mutagenesis and restriction endonuclease selection (Deng and Nickoloff, 1992). An M9L mutation was introduced by the same method into a frog *Xrx1* cDNA clone in the pSP64RI vector (kindly provided by Pete Mathers). Full-length mouse *Rx* expression constructs were created in pCS2 by ligating *Xba*I-*Bsr*GI fragments from 5′ and 3′ cDNA clones (Mathers *et al.,* 1997). To determine the exact site of translation initiation, a panel of mutant and wild-type *Rx*-myc fusion constructs was created in pCS2MT (Rupp *et al.,* 1994; Turner and Weintraub, 1994). The expression cassettes contain 86 bp of 5′UTR and the 66 amino-terminal codons of mouse *Rx*, followed in frame by six tandem Myc epitopes, and are transcribed in vivo from the simian CMV promoter. Fusion polypeptides starting at codons M1 or M10 contain 166 or 157 amino acids, respectively. The fusion constructs also contain an optimal translation initiation sequence (AAAGCTATGG) at M73 within the pCS2MT vector.

Cell Culture and Protein Analysis

Translation initiation was studied *in vivo* using 293T human embryonic kidney cells. Cultures were transfected with pCS2(*Rx*-myc) or control pCS2MT plasmids by $CaPO_4$ co-precipitation (2.5 μg per 60-mm dish). After 48 h, whole-cell extracts were harvested in cold lysis buffer (50 mM Tris, 150 mM NaCl, 1% NP40, pH 8.0) and clarified by centrifugation. To resolve fusion proteins in the size range between 17 and 19 kDa, supernatants were electrophoresed through a 14-cm 18% polyacrylamide gel for 10 h at 14 V/cm. The gel buffer was 350 mM Bis-Tris, pH 6.5 and the running buffer was 50 mM MOPS, 50 mM Tris, 0.1% SDS, 1 mM EDTA, pH 7.7. Myc-tagged proteins were detected in Western blots using 9E10 monoclonal antibody (1:200), HRP-conjugated sheep anti-mouse IgG (1:20,000, Amersham), and enhanced chemiluminescence (ECL) reagents (Renaissance, NEN). To confirm the interpretation of migration patterns, selected cell extracts from mutant and control transfections were mixed and co-electrophoresed. Similar results were obtained for pCS2(*Rx*-myc) constructs in three different transfection experiments. To verify that an equivalent amount of cell extract was loaded in each lane and control for transfection efficiency, we probed nitrocellulose filters with a monoclonal antibody (DM1A) that detects endogenous α-tubulin (1:200, Neomarkers) or co-transfected a plasmid encoding an unrelated Myc-tagged protein.

To assess the efficiency of Rx translation overall, duplicate 60-mm cultures of Ad12 HER10 human embryonic retinal cells (Grabham *et al.,* 1988) were co-transfected in parallel with 1.0 μg of the full-length mutant or wild-type *Rx* expression constructs or pCS2 vector. Plasmid DNAs were introduced using FuGENE6 reagent (Roche). After 60 h, soluble proteins were extracted from cells by lysis in cold RIPA buffer (150 mM NaCl, 1.0% NP40, 0.5% deoxycholate, 0.1% SDS, 50 mM Tris, pH 8.0) and electrophoresed through 10% polyacrylamide SDS Bis-Tris gels (Novex, 20 μg per lane). After transfer, Western blots were probed in series with polyclonal rabbit anti-RX IgG (1:200) and DM1A (α-tubulin). The anti-RX IgG was purified from whole rabbit serum (Kimura *et al.,* 2000). Primary antibodies were detected using HRP-protein A (1:5,000, KPL) or HRP-conjugated sheep anti-mouse IgG (1:20,000, Amersham) and ECL reagents (NEN). The relative abundance of Rx protein was determined by densitometry from multiple ECL exposures. The *Rx* mRNA levels in transfected cells were equivalent by RT-PCR.

Xenopus RNA Microinjection

Capped RNA from wild-type and M9L mutant *Xrx1* cDNA clones was synthesized in vitro using SP6 polymerase (Ambion) and microinjected using standard techniques (Kanekar *et al.,* 1997) into one of two D.1 blastomeres in 8-cell *Xenopus* embryos. These dorsal blastomeres normally form retinae, brain, and other anterior structures (Bauer *et al.,* 1994). The injected *Xrx1*

transcripts contain rabbit β-globin UTR sequences but are not polyadenylated. We tested a range of *Xrx1* RNA amounts from 50 to 200 pg and co-injected a β-gal tracer RNA (50 pg). Similar experiments were performed using 10 to 68 pg capped mouse *Rx* RNA derived from wild-type, M1L, M10L, M1★, M10★ and M1★/M10L clones in pCS2 (Rupp *et al.,* 1994; Turner and Weintraub, 1994); these transcripts contain an SV40 polyA cassette that can be utilized by injected *Xenopus* embryos, leading to significantly higher levels of protein expression (D.L. Turner, personal communication). Embryos were stained for β-galactosidase at stage 39–41 and evaluated under the dissection microscope and by histology. Toxicity was assessed by comparing the extent of staining in embryos co-injected with *Rx* and β-gal RNAs to embryos injected with β-gal RNA alone. Abnormal phenotypes were assessed in comparison with the contralateral uninjected sides as described (Mathers *et al.,* 1997).

GenBank Accession Numbers

Mus musculus Rx/rax genomic DNA, AF319462 and AF319461; *Mus musculus Rx/rax* cDNA, AF001906 and U73177; *Rattus norvegicus Rx* genomic DNA, AF320224 and AF320225; *Rattus norvegicus Rx* cDNA AF135839; *Homo sapiens RX* cDNA, AF115392; *Xenopus laevis Xrx1* cDNA, AF017273 and AF001048; *Xenopus laevis Xrx2* cDNA, AF001049; *Gallus gallus cRx2/cRax2* cDNA, AF092538; *Danio rerio Zrx1* cDNA, AF001907; *Danio rerio Zrx2* cDNA, AF001908; *Danio rerio Zrx3* cDNA, AF001909; *Astyanax mexicanus Rx1* cDNA, AF264703; *Oryzias latipes Rx2* cDNA, AJ007939.

ACKNOWLEDGMENTS

We thank Ursula Drager, Neil Gonsalves, and Boris Konyukhov for providing ZRDCT mice; Pete Mathers for *Rx* cDNA clones; David Turner for pCS2 vectors and advice; Toshi Shinohara for anti-RX antisera; Phil Gallimore for HER10 cells; Richard Sage for wild-caught *Mus* DNA samples; Chuan-Min Chen for technical assistance; Karen Rader for historical advice regarding C.C. Little and the origins of ZRDCT mice; Ursula Drager, Pete Mathers, Jerry Silver, David Ginsburg, Pam Raymond, John Moran, Kevin Patrie, Ben Margolis, and Charles Mitchell for helpful advice; and Miriam Meisler, Margit Burmeister, and Sally Camper for critically reading the manuscript. This work was supported by grants from the NSF to PKT, from the NIH and Howard Hughes Medical Institute to TG, from Research to Prevent Blindness; Inc. to LL, and from the NIH and Pew Charitable Trusts to MV.

LITERATURE CITED

Andreazzoli M, Gestri G, Angeloni D, Menna E, Barsacchi G. 1999. Role of Xrx1 in Xenopus eye and anterior brain development. Development 126:2451–2460.

Bateman JB. 1984. Microphthalmos. Int Ophthalmol Clin 24:87–107.

Bauer DV, Huang S, Moody SA. 1994. The cleavage stage origin of Spemann's Organizer: Analysis of the movements of blastomere clones before and during gastrulation in Xenopus. Development 120:1179–1189.

Beck JA, Lloyd S, Hafezparast M, Lennon-Pierce M, Eppig JT, Festing MF, Fisher EM. 2000. Genealogies of mouse inbred strains. Nat Genet 24:23–25.

Beck SL. 1963. The anophthalmic mutant of the mouse I. Genetic contribution to the anophthalmic phenotype. J Hered 54:39–44.

Bernier G, Panitz F, Zhou X, Hollemann T, Gruss P, Pieler T. 2000. Expanded retina territory by midbrain transformation upon overexpression of six6 (Optx2) in xenopus embryos. Mech Dev 93: 59–69.

Bone-Larson C, Basu S, Radel JD, Liang M, Perozek T, Kapousta-Bruneau N, Green DG, Burmeister M, Hankin MH. 2000. Partial rescue of the ocular retardation phenotype by genetic modifiers. J Neurobiol 42:232–247.

Breitman ML, Clapoff S, Rossant J, Tsui LC, Glode LM, Maxwell IH, Bernstein A. 1987. Genetic ablation: Targeted expression of a toxin gene causes microphthalmia in transgenic mice. Science 238:1563–1565.

Brown NL, Kanekar S, Vetter ML, Tucker PK, Gemza DL, Glaser T. 1998. Math5 encodes a murine basic helix-loop-helix transcription factor expressed during early stages of retinal neurogenesis. Development 125:4821–4833.

Burmeister M, Novak J, Liang MY, Basu S, Ploder L, Hawes NL, Vidgen D, Hoover F, Goldman D, Kalnins VI, Roderick TH, Taylor BA, Hankin MH, McInnes RR. 1996. Ocular retardation mouse caused by Chx10 homeobox null allele: Impaired retinal progenitor proliferation and bipolar cell differentiation. Nat Genet 12:376–384.

Casarosa S, Andreazzoli M, Simeone A, Barsacchi G. 1997. Xrx1, a novel Xenopus homeobox gene expressed during eye and pineal gland development. Mech Dev 61:187–198.

Chang B, Smith RS, Hawes NL, Anderson MG, Zabaleta A, Savinova O, Roderick TH, Heckenlively JR, Davisson MT, John SW. 1999. Interacting loci cause severe iris atrophy and glaucoma in DBA/2J mice. Nat Genet 21:405–409.

Chase HB. 1942. Studies on an anophthalmic strain of mice. III. Results of crosses with other strains. Genetics 27:339–348.

Chase HB. 1944. Studies on an anophthalmic strain of mice. IV. A second major gene for anophthalmia. Genetics 29:264–269.

Chase HB. 1945. Studies on an anophthalmic strain of mice. V. Associated cranial nerves and brain centers. J Comp Neurol 83:121–139.

Chase HB. 1949. Mouse News Lett 1:11–12.

Chase HB, Chase EB. 1941. Studies of an anophthalmic strain of mice. I. Embryology of the eye region. J Morph 68:279–301.

Cheadle JP, Belloni E, Ferrari M, Millar-Jones L, Meredith AL. 1994. A novel mutation (M1V) in the translation initiation codon of the cystic fibrosis transmembrane conductance regulator gene, in three CF chromosomes of Italian origin. Hum Mol Genet 3:1431–1432.

Choong CS, Quigley CA, French FS, Wilson EM. 1996. A novel missense mutation in the amino-terminal domain of the human androgen receptor gene in a family with partial androgen insensitivity syndrome causes reduced efficiency of protein translation. J Clin Invest 98:1423–1431.

Chuang JC, Mathers PH, Raymond PA. 1999. Expression of three Rx homeobox genes in embryonic and adult zebrafish. Mech Dev 84:195–198.

Cooper HM, Herbin M, Nevo E. 1993. Visual system of a naturally microphthalmic mammal: The blind mole rat, Spalax ehrenbergi. J Comp Neurol 328:313–350.

Cornelis S, Bruynooghe Y, Denecker G, Van Huffel S, Tinton S, Beyaert R. 2000. Identification and characterization of a novel cell cycle-regulated internal ribosome entry site. Mol Cell 5:597–605.

Deng WP, Nickoloff JA. 1992. Site-directed mutagenesis of virtually any plasmid by eliminating a unique site. Anal Biochem 200:81–88.

Deschet K, Bourrat F, Ristoratore F, Chourrout D, Joly JS. 1999. Expression of the medaka (Oryzias latipes) Ol-Rx3 paired-like gene in two diencephalic derivatives, the eye and the hypothalamus. Mech Dev 83:179–182.

Dietrich WF, Miller JC, Steen RG, Merchant M, Damron D, Nahf R, Gross A, Joyce DC, Wessel M, Dredge RD, Marquis A, Stain LD,

Goodman N, Page DC, Lander ES, 1994. A genetic map of the mouse with 4,006 simple sequence length polymorphisms. Nat Genet 7:220–245.

Duke-Elder S. 1964. Congenital deformities of the eye. I. Anomalies in organogenesis. St. Louis, MO: CV Mosby. p 415–428.

Eggert T, Hauck B, Hildebrandt N, Gehring WJ, Walldorf U. 1998. Isolation of a Drosophila homolog of the vertebrate homeobox gene Rx and its possible role in brain and eye development. Proc Natl Acad Sci USA 95:2343–2348.

Faradji-Prevautel H, Cespuglio R, Jouvet M. 1990. Circadian rest-activity rhythms in the anophthalmic, monocular and binocular ZRDCT/An mice. Retinal and serotoninergic (raphe) influences. Brain Res 526:207–216.

Ferda Percin E, Ploder LA, Yu JJ, Arici K, Jonathan Horsford D, Rutherford A, Bapat B, Cox DW, Duncan AM, Kalnins VI, Kocak-Altintas A, Sowden JC, Traboulsi E, Sarfarazi M, McInnes RR. 2000. Human microphthalmia associated with mutations in the retinal homeobox gene CHX10. Nat Genet 25:397–401.

Furukawa T, Kozak CA, Cepko CL. 1997. rax, a novel paired-type homeobox gene, shows expression in the anterior neural fold and developing retina. Proc Natl Acad Sci USA 94:3088–3093.

Godement P, Saillour P, Imbert M. 1979. Thalamic afferents to the visual cortex in congenitally anophthalmic mice. Neurosci Lett 13:271–278.

Grabham PW, Grand RJA, Byrd PJ, Gallimore PH. 1988. Differentiation of normal and adenovirus-12 E1 transformed human embryo retinal cells. Exp Eye Res 47:123–133.

Grenier JK, Carroll SB. 2000. Functional evolution of the Ultrabithorax protein. Proc Natl Acad Sci USA 97:704–709.

Hann SR, King MW, Bentley DL, Anderson CW, Eisenman RN. 1988. A non-AUG translational initiation in c-myc exon 1 generates an N-terminally distinct protein whose synthesis is disrupted in Burkitt's lymphomas. Cell 52:185–195.

Harch C, Chase HB, Gonsalves NI. 1978. Studies on an anophthalmic strain of mice. VI. Lens and cup interaction. Dev Biol 63:352–357.

Hill RE, Favor J, Hogan BL, Ton CC, Saunders GF, Hanson IM, Prosser J, Jordan T, Hastie ND, van Heyningen V. 1991. Mouse small eye results from mutations in a paired-like homeobox-containing gene. Nature 354:522–525.

Hodgkinson CA, Moore KJ, Nakayama A, Steingrimsson E, Copeland NG, Jenkins NA, Arnheiter H. 1993. Mutations at the mouse microphthalmia locus are associated with defects in a gene encoding a novel basic-helix-loop-helix-zipper protein. Cell 74:395–404.

Johnson KR, Lane PW, Ward-Bailey P, Davisson MT. 1995. Mapping the mouse dactylaplasia mutation, Dac, and a gene that controls its expression, mdac. Genomics 29:457–464.

Kajiwara K, Berson EL, Dryja TP. 1994. Digenic retinitis pigmentosa due to mutations at the unlinked peripherin/RDS and ROM1 loci. Science 264:1604–1608.

Kanekar S, Perron M, Dorsky R, Harris WA, Jan LY, Jan YN, Vetter ML. 1997. Xath5 participates in a network of bHLH genes in the developing Xenopus retina. Neuron 19:981–994.

Katz MJ, Lasek RJ, Kaiserman-Abramof IR. 1981. Ontophyletics of the nervous system: Eyeless mutants illustrate how ontogenetic buffer mechanisms channel evolution. Proc Natl Acad Sci USA 78:397–401.

Kimura A, Singh D, Wawrousek EF, Kikuchi M, Nakamura M, Shinohara T. 2000. Both PCE-1/RX and OTX/CRX interactions are necessary for photoreceptor-specific gene expression. J Biol Chem 275: 1152–1160.

Kohn G, el Shawwa R, el Rayyes E. 1988. Isolated "clinical anophthalmia" in an extensively affected Arab kindred. Clin Genet 33:321–324.

Koniukhov BV, Iakovlev MI. 1986. [Expression of mutant eyeless genes in the mouse embryo retina]. Biull Eksp Biol Med 101:738–740.

Konyukhov BV, Malinina NA, Platonov ES, Yakovlev MI. 1978. Immunohistochemical study of crystallin synthesis during morphogenesis of the crystalline lens in mice. Biol Bull Acad Sci USSR 5:397–405.

Kozak M. 1990. Downstream secondary structure facilitates recognition of initiator codons by eukaryotic ribosomes. Proc Natl Acad Sci USA 87:8301–8305.

Kozak M. 1995. Adherence to the first-AUG rule when a second AUG codon follows closely upon the first. Proc Natl Acad Sci USA 92:7134.

Kozak M. 1996. Interpreting cDNA sequences: Some insights from studies on translation. Mamm Genome 7:563–574.

Laemle LK, Ottenweller JE. 1998. Daily patterns of running wheel activity in male anophthalmic mice. Physiol Behav 64:165–171.

Laemle LK, Rusa R. 1992. VIP-like immunoreactivity in the suprachiasmatic nuclei of a mutant anophthalmic mouse. Brain Res 589:124–128.

Liu Y, Garceau NY, Loros JJ, Dunlap JC. 1997. Thermally regulated translational control of FRQ mediates aspects of temperature responses in the neurospora circadian clock. Cell 89:477–486.

Markussen FH, Michon AM, Breitwieser W, Ephrussi A. 1995. Translational control of oskar generates short OSK, the isoform that induces pole plasma assembly. Development 121:3723–3732.

Mathers PH, Grinberg A, Mahon KA, Jamrich M. 1997. The Rx homeobox gene is essential for vertebrate eye development. Nature 387:603–607.

Ochman H, Medhora MM, Garza D, Hartl DL. 1990. Amplification of flanking sequences by inverse PCR. In: Innis M, Gelfand D, Sninsky J, White T, editors. San Diego: Academic Press. p 219–227.

Ohuchi H, Tomonari S, Itoh H, Mikawa T, Noji S. 1999. Identification of chick rax/rx genes with overlapping patterns of expression during early eye and brain development. Mech Dev 85:193–195.

Olavarria J, van Sluyters RC. 1984. Callosal connections of the posterior neocortex in normal-eyed, congenitally anophthalmic, and neonatally enucleated mice. J Comp Neurol 230:249–268.

Olson MV. 1999. When less is more: Gene loss as an engine of evolutionary change. Am J Hum Genet 64:18–23.

Pierro LJ, Spiggle J. 1967. Congenital eye defects in the mouse. I. Corneal opacity in C57black mice. J Exp Zool 166:25–33.

Rhoades RW, Mooney RD, Fish SE. 1985. Subcortical projections of area 17 in the anophthalmic mouse. Brain Res 349:171–181.

Robinson ML, Holmgren A, Dewey MJ. 1993. Genetic control of ocular morphogenesis: Defective lens development associated with ocular anomalies in C57BL/6 mice. Exp Eye Res 56:7–16.

Rupp RA, Snider L, Weintraub H. 1994. Xenopus embryos regulate the nuclear localization of XMyoD. Genes Dev 8:1311–1323.

Sedman SA, Mertz JE. 1988. Mechanisms of synthesis of virion proteins from the functionally bigenic late mRNAs of simian virus 40. J Virol 62:954–961.

Sidow A, Bulotsky MS, Kerrebrock AW, Bronson RT, Daly MJ, Reeve MP, Hawkins TL, Birren BW, Jaenisch R, Lander ES. 1997. Serrate2 is disrupted in the mouse limb-development mutant syndactylism. Nature 389:722–725.

Silver J. 1977. Abnormal development of the suprachiasmatic nuclei of the hypothalamus in a strain of genetically anophthalmic mice. J Comp Neurol 176:589–606.

Silver J, Hughes AF. 1974. The relationship between morphogenetic cell death and the development of congenital anophthalmia. J Comp Neurol 157:281–301.

Silver J, Puck SM, Albert DM. 1984. Development and aging of the eye in mice with inherited optic nerve aplasia: Histopathological studies. Exp Eye Res 38:257–266.

Smith RS, Roderick TH, Sundberg JP. 1994. Microphthalmia and associated abnormalities in inbred black mice. Lab Anim Sci 44:551–560.

Snell GD. 1941. Inbred strains. Mouse Genetic News 1:9.

Taylor BA, Navin A, Phillips SJ. 1994. PCR-amplification of simple sequence repeat variants from pooled DNA samples for rapidly mapping new mutations of the mouse. Genomics 21:626–632.

Tsujino S, Rubin LA, Shanske S, DiMauro S. 1994. An A-to-C substitution involving the translation initiation codon in a patient with myophosphorylase deficiency (McArdle's disease). Hum Mutat 4:73–75.

Turner DL, Weintraub H. 1994. Expression of achaete-scute homolog 3 in Xenopus embryos converts ectodermal cells to a neural fate. Genes Dev 8:1434–1447.

Voronina VA, Mathers PH. 2000. Mutations in the human RX gene in a patient with anophthalmia. Invest Ophthalmol Vis Sci 41:S32.

Waye JS, Eng B, Patterson M, Barr RD, Chui DH. 1997. De novo mutation of the beta-globin gene initiation codon (ATG→AAG) in a Northern European boy. Am J Hematol 56:179–182.

Webster EH Jr., Silver AF, Gonsalves NI. 1984. The extracellular matrix between the optic vesicle and presumptive lens during lens morphogenesis in an anophthalmic strain of mice. Dev Biol 103:142–150.

Wilkens H. 1971. Genetic interpretation of regressive evolutionary processes: Studies on hybrid eyes of two Astyanax cave populations (Characidae, Pisces). Evolution 25:530–544.

Wright S. 1968. Evolution and the genetics of populations. Vol. I. Genetic and biometric foundations. Chicago: The University of Chicago Press.

Yamamoto Y, Jeffery WR. 2000. Central role for the lens in cave fish eye degeneration. Science 289:631–633.

Zhang L, Mathers PH, Jamrich M. 2000. Function of Rx, but not Pax6, is essential for the formation of retinal progenitor cells in mice. Genesis 28:135–142.

Zwaan J, Silver J. 1983. Crystallin synthesis in the lens rudiment of a strain of mice with congenital anophthalmia. Exp Eye Res 36:551–557.